

Laser-Induced Breakdown Spectroscopy of High-Pressure Bulk Aqueous Solutions

MARION LAWRENCE-SNYDER, JON SCAFFIDI, S. MICHAEL ANGEL,*
ANNA P. M. MICHEL, and ALAN D. CHAVE

Department of Chemistry and Biochemistry, University of South Carolina, Columbia, South Carolina 29208 (M.L.-S., J.S., S.M.A.);
Massachusetts Institute of Technology/Woods Hole Oceanographic Institution Joint Program Department of Applied Ocean Physics and
Engineering, Woods Hole Oceanographic Institution, MS#7, Woods Hole, Massachusetts 02543 (A.P.M.M.); and Department of Applied Ocean
Physics and Engineering, Woods Hole Oceanographic Institution, MS#7, Woods Hole, Massachusetts 02543 (A.D.C.)

Laser-induced breakdown spectroscopy (LIBS) is presented for detection of several Group I and II elements (e.g., Na, Ca, Li, and K), as well as Mn and CaOH, in bulk aqueous solution at pressures exceeding 2.76×10^7 Pa (276 bar). Preliminary investigations reveal only minor pressure effects on the emission intensity and line width for all elements examined. These effects are found to depend on detector timing and laser pulse energy. The results of these investigations have implications for potential applications of LIBS for *in situ* multi-elemental detection in deep-ocean environments.

Index Headings: Laser-induced breakdown spectroscopy; LIBS; Plasma; Hydrothermal vent; High pressure; Bulk solution.

INTRODUCTION

Hydrothermal vent activity at mid-ocean ridges has an influence on all aspects of oceanography (e.g., seawater chemistry, oceanic crust composition, and communities of chemosynthetic organisms), and the influence even extends beyond the ocean to the atmosphere.¹ However, the magnitude and importance of these effects have not been quantified due, in part, to the complex nature of the environment and the lack of available sensors.^{1,2} Analysis of hydrothermal vent fluids, issuing from the seafloor at depths of more than several kilometers, is particularly challenging due to the high pressure (200–300 bar) and harsh thermal (typical orifice temperatures of 350 °C) and corrosive (e.g., low pH, high sulfide, high metal, volatile-rich) environment.^{2,3} Since the initial discovery of the first hydrothermal vent on an ocean ridge crest, in 1977, samples have been taken and analyzed using sophisticated shore-based methods.⁴ However, these methods not only lead to sampling problems (e.g., mixing of hydrothermal vent fluid with surrounding seawater, perturbation of the environment, and changes in the physical and chemical composition of fluid samples when removed from the high pressure/temperature conditions of the vents), but also limit the ability to provide the sustained, high-resolution and high-frequency measurements that are necessary for understanding the global impact of the variable and dynamic physical, chemical, and biological processes of hydrothermal vent activity.^{2,3} For these reasons, an *in situ* sensor capable of real-time, noninvasive, time-series measurements with high temporal and spatial resolution would be a significant advancement over current oceanographic technology.^{2,3}

Laser-induced breakdown spectroscopy (LIBS), first reported by Brech and Cross in 1962,⁵ is a relatively simple *in situ* spectroscopic technique that has the potential to provide

the sustained, high-frequency measurements that are required to investigate the dynamic nature of hydrothermal vent fluids. Besides the ability to identify and quantify the elemental composition of materials in the solid, liquid, and gaseous state with little or no sample preparation, LIBS is also one of the few techniques capable of non-contact and remote analysis,^{6–22} making it particularly useful for applications where analysis must be carried out in extreme or hostile environments.^{14–21,23–31}

Despite the obvious potential of LIBS for oceanographic applications, there are very few reports of LIBS for underwater (in-bulk) analysis.^{22,32–47} The limited attention may be attributed, in part, to the difficulties of LIBS for in-bulk analysis, including significant reduction in plasma emission intensity caused by strong quenching by the dense liquid matrix^{33,35,43,44,47} and spectral line broadening due to increased collisions and Stark broadening effects.^{32,33,41–43,47,48} Additionally, only emission lines corresponding to lower energy excited states and those with longer durations than the continuum emission can be detected^{32,34,39,42–44} because of rapid recombination and plasma cooling (plasma emission lifetimes are usually very short, on the order of 1 μ s or less^{32,34–36,43,47} compared to typical lifetimes of 5–20 μ s observed in ambient air^{35,49,50}).

Due to the fact that relatively few in-bulk LIBS studies have been performed, the effects of many important analytical parameters such as laser excitation characteristics (e.g., wavelength, power, pulse duration, and pulse rate), detector timing, and experimental conditions related to the surrounding environment (fluid composition, turbidity, pressure, and temperature) have not been fully addressed. The work described in this paper is motivated by the desire to gain fundamental knowledge concerning the effect of pressure on LIBS measurements of bulk solution, and ultimately to determine the suitability of LIBS for *in situ* analysis of hydrothermal vent fluids. This paper extends previous work^{38,39} to the measurement of bulk aqueous solutions at high pressures (exceeding 2.76×10^7 Pa, 276 bar) and briefly addresses several of the important issues for LIBS of high-pressure bulk aqueous solutions. To the best of our knowledge, this is the first report of LIBS for analysis of aqueous solutions at pressures comparable to those at deep-ocean hydrothermal vents.

EXPERIMENTAL

The basic LIBS experimental setup is shown in Fig. 1. Sample solutions were analyzed in a high-pressure steel sample chamber (see insert in Fig. 1) constructed of SS 316 stainless steel Swagelok fittings (Central Swagelok Company, Solon,

Received 9 February 2006; accepted 19 April 2006.

* Author to whom correspondence should be sent. E-mail: angel@mail.chem.sc.edu.

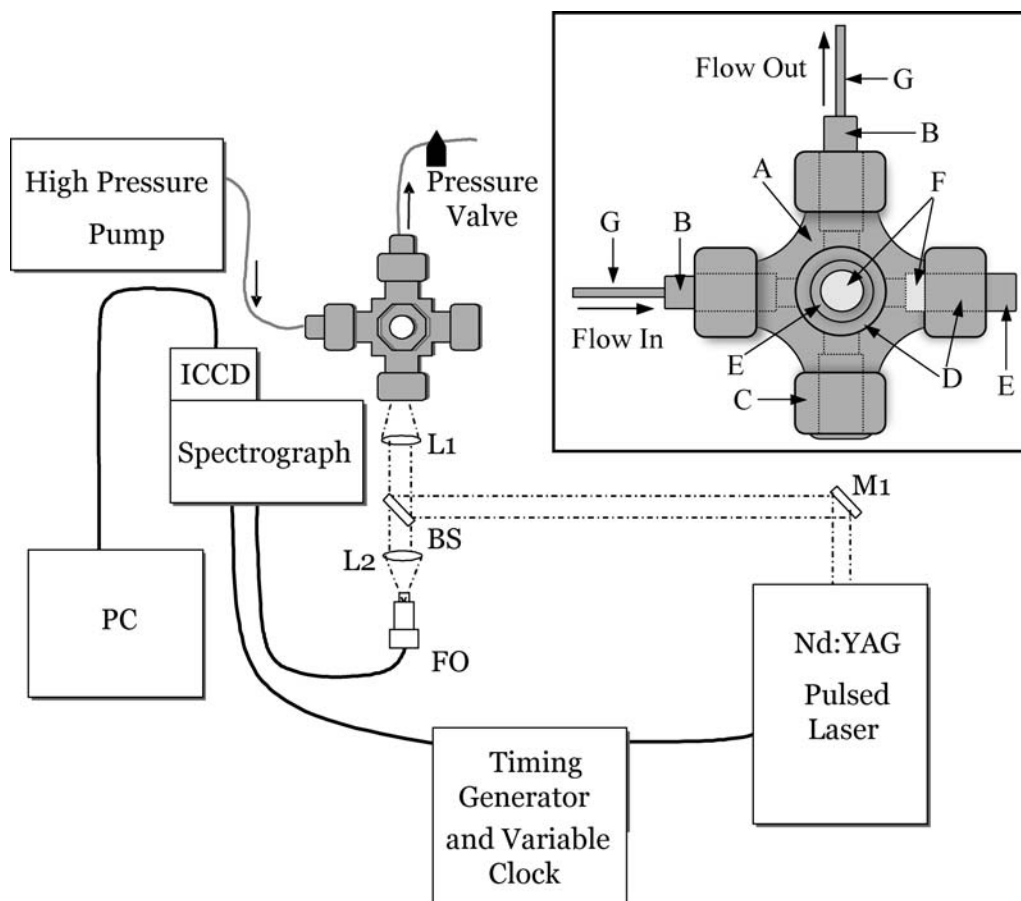


FIG. 1. Schematic diagram of the LIBS apparatus. The labels L, M, BS, and FO symbolize lens, mirror, beamsplitter, and fiber-optic, respectively. (Inset) Labeled schematic of high-pressure cell: (A) 6-port sample chamber, (B) reducer, (C) lug, (D) female hex nut, (E) 25.4-mm-o.d. and 19.05-mm-i.d. tubing, (F) circular sapphire windows, and (G) 3.175 mm tubing.

OH). The sample chamber was assembled by welding two additional ports to a 25.4-mm-i.d. Union cross (SS-1610-4), forming six identical 25.4 mm tube ports. Stainless steel plugs were used to seal the unused ports, and reducers coupled with female hex nuts were used to attach 3.175 mm stainless steel tubing to two of the chamber ports, in order to allow solution flow into the cell from the high pressure pump (Isco Syringe Pump Model 260D, Teledyne Technologies Incorporated) and out of the cell to a high pressure valve. Sapphire windows with 25.4 mm diameter and 3.175 mm or 6.35 mm thickness (MSW100/125, Meller Optics Incorporated, Providence, RI) were affixed in the cell using female hex nuts and 25.4 mm long pieces of 25.4-mm-o.d., 19.05-mm-i.d. tubing.

The Nd:YAG laser pulses (Continuum Surelite III, 5-ns pulse or Quantel Nd 580 laser, 9 ns pulse; 1064 nm, 5 Hz) were focused into the sample chamber using the mirror and lens arrangement shown in Fig. 1. Plasma emission was collected collinear with the path of the laser pulses to ensure optimal overlap between the collection field of view and the laser-induced plasma, and was focused onto an optical fiber for transmission to a spectrograph/detector system. A variable clock (Stanford Instruments Model SR250) with a delay generator (Stanford Instruments Model DG535) was used to trigger the laser and collection electronics and to allow control of important timing parameters, including the detector gate delay, t_d (the time interval before measurement begins following the laser pulse), and detector gate width, t_b (the

time during which the emission is integrated). These timing parameters, as well as other system parameters, were not fully optimized as part of our investigations, but were chosen based on preliminary observations to provide relatively intense elemental line emission while minimizing background continuum emission. For simplicity, the minimum detector delay value, t_d , used in this investigation is reported as 0 μ s. This delay actually corresponds to the earliest time (approximately 200 ns following the laser pulse) that emission could be recorded, while avoiding detector saturation. Therefore, all reported t_d values are offset by 200 ns.

For maximum throughput and higher signal intensities, a Chromex spectrograph (Model 250IS/RF; 0.25 m, $f/4$) with a 1200 groove grating blazed at 500 nm and a slit width of 25 μ m (providing 0.0625 nm spectral resolution), coupled to a 2 mm core diameter, 0.51 NA, light guide (Edmund Scientific Co. Model O2551), and an intensified charge-coupled device (ICCD) camera (Princeton Instruments I-Max 1024E), controlled with WinSpec/32 version 2.5.7.3 software and a pulse timing generator (Roper Scientific ST-133A), was used for collection and detection, respectively. Spectra were averaged over 10 replicate measurements, each the sum of 250 accumulations (i.e., 250 pulses), with a gain of 255.

For maximum spectral coverage (200–780 nm), an echellette spectrograph (Echelle Spectra Analyzer ESA 3000EV, LLA Instruments GmbH, Berlin; 0.25 m, $f/10$) coupled with an 800 μ m core diameter, 0.22 NA, 1.5 m long fused silica optical

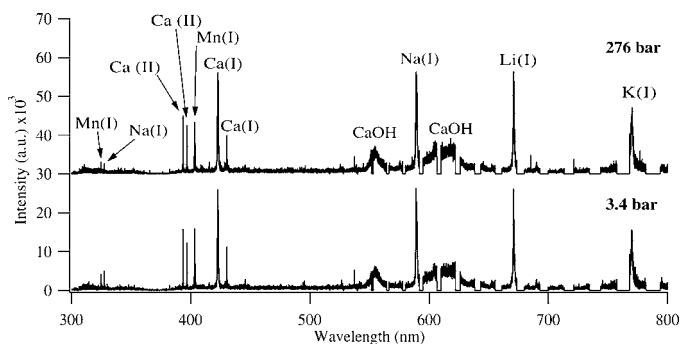


Fig. 2. Comparison of LIBS spectra of a solution containing 5000 ppm K, Ca, and Mn, 1000 ppm Li, and trace amount of Na at low (3.4×10^5 Pa, 3.4 bar) (lower trace) and high (2.76×10^7 Pa, 276 bar) pressure (upper trace). Spectra were acquired using the Echelle system. Atomic, ionic, and molecular emission lines/bands are labeled. Laser pulse energy = 60 mJ/pulse, $t_d = 200$ ns, and $t_b = 100$ ns. The upper trace has been offset for clarity.

fiber (Polymicro Technologies, P/N 6101843) and a CCD array coupled with an MCP-image intensifier (Model 3000 CP) controlled via a fast-pulse-generator and driver board were used for collection and detection, respectively. The standard 38 μm wide slit was replaced with a custom 100 μm wide slit to increase the light throughput by a factor of 2.6, with a resulting 1.6-fold decrease in spectral resolution (10 to 50 μm over the 200–780 nm spectral range of the instrument). A 10 cm focal length off-axis aluminum coated parabolic mirror (Janos Technology Model A8037–113) was used in place of the collection lens, L_2 (see Fig. 1), to reduce wavelength-dependent focal length changes over the wide spectral range of the Echelle system. Spectra were acquired using ESAWIN version 3.16 software and are the average of five replicate measurements, each the sum of 100 on-chip accumulations, with an MCP amplification of 3700. A detailed evaluation of this Echelle spectrometer for LIBS measurements has been described.⁵¹

Samples were prepared using chloride or bromide salts (except for manganese, which was prepared using manganous sulfate) dissolved in deionized water. Concentrations were chosen to provide relatively intense analyte emission while avoiding detector saturation and are reported as parts per million (ppm wt./wt.). Analyte emission intensities were calculated after baseline subtraction, and line widths were calculated by fitting the peaks using a macro in IGOR and measuring the half-width (full-width at half-maximum, FWHM) of the fitted curve. Limits of detection were calculated using the emission line intensity for the element of interest at a known concentration. Assuming that emission intensity decreases linearly with concentration, the detection limit was estimated as the concentration that would produce an emission intensity equal to twice the standard deviation of the background signal.

RESULTS

To the best of our knowledge, LIBS has not previously been used to analyze bulk solutions at elevated pressures. Therefore, the first goal of these investigations was to determine the feasibility of LIBS for measuring dissolved analytes at pressures corresponding to the depths of hydrothermal vents (i.e., 200–300 bar). Initial studies were performed using the rapid multi-elemental detection capabilities of the Echelle

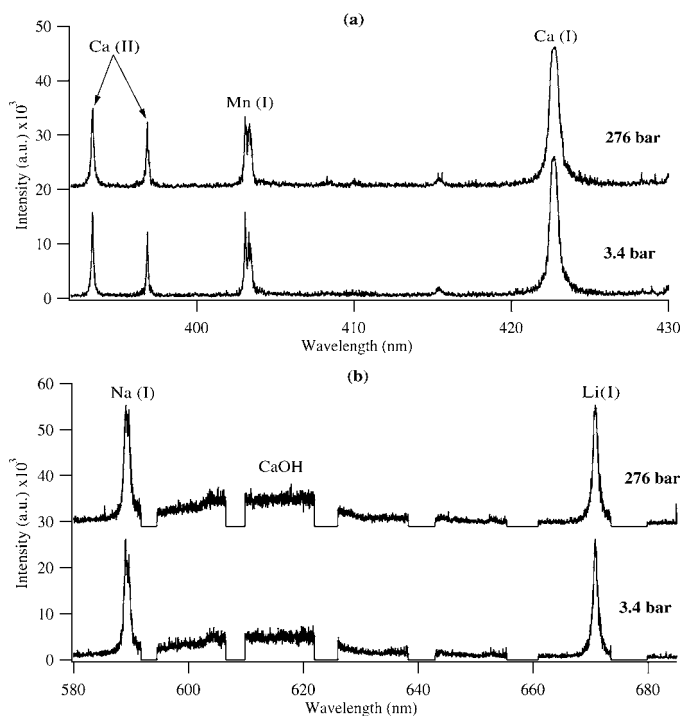


Fig. 3. Enlarged spectral regions from Fig. 2 showing (a) Ca(II) (393.366 and 396.847 nm), Mn(I) (403.076, 403.307, and 403.449 nm), and Ca(I) (422.673 nm) emission, and (b) Na(I) (588.995 and 589.592 nm), CaOH (broad feature around 608–623 nm), and Li(I) (670.776 and 670.791 nm) emission at low (3.4×10^5 Pa, 3.4 bar) (lower trace) and high (2.76×10^7 Pa, 276 bar) pressure (upper trace). Upper traces have been offset for clarity.

system, allowing simultaneous measurement of many species that are found in hydrothermal vent fluids (Li, Na, K, Ca, Mn). These species were selected from a larger list¹ because they are easily measured using LIBS. Figure 2 shows Echelle spectra over the 300 to 780 nm wavelength range for an aqueous solution containing 5000 ppm K, Mn, and Ca, 1000 ppm Li, and trace amounts of Na at low (3.4×10^5 Pa, 3.4 bar) and high pressure (2.76×10^7 Pa, 276 bar). Similar spectra were successfully acquired at pressures exceeding 320 bar. Selected spectral regions from Fig. 2 are shown expanded in Figs. 3a and 3b in order to show line widths and intensities more clearly. Intense atomic (I) and ionic (II) lines, as well as molecular CaOH bands, are labeled. The Mn(I) triplet (403.076, 403.307, and 403.449 nm) and Na(I) (588.995 and 589.592 nm) and Li(I) (670.776 and 670.791 nm) doublets (see Figs. 3a and 3b) are not completely resolved due to increased collisions and Stark broadening effects caused by the dense aqueous medium.^{32,37,41–43} It should also be noted that the Echelle mode of dispersion involves the loss of zones of the spectrum located between the different orders, leading to the gaps seen in these spectra.⁵¹ Surprisingly, the spectra shown in Figs. 2 and 3 reveal little, if any, pressure effect on line width or intensity for the dissolved species that were studied.

The data shown in Figs. 2 and 3 seems to show that pressure has no significant effect on emission intensity or line width; however, this is not always true. Pressure is shown to have a pronounced effect on the in-bulk LIBS emission when different experimental conditions are used (e.g., different laser powers and detector gate delays). Figure 4 shows the temporal dependence of the unresolved Li(I) doublet (670.776 and 670.791 nm) emission, for an aqueous solution containing

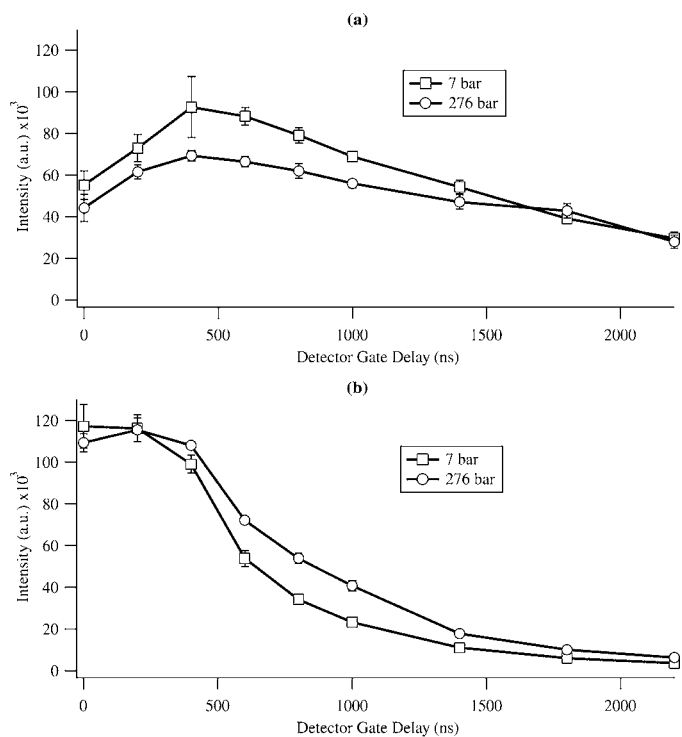


FIG. 4. Temporal dependence ($t_d = 0$ –2200 ns) of the Li(I) doublet (670.776 and 670.791 nm) emission intensity at (□) low (7×10^5 Pa, 7 bar) and (○) high (2.76×10^7 Pa, 276 bar) pressure for pulse energies of (a) 30 mJ/pulse and (b) 60 mJ/pulse. Measurements were made using the Chromex system and $t_b = 1$ μ s. Error bars represent 1 standard deviation.

1000 ppm Li at low (7×10^5 Pa, 7 bar) and high pressure (2.76×10^7 Pa, 276 bar), using laser pulse energies of 30 (Fig. 4a) and 60 mJ/pulse (Fig. 4b). For these measurements, the Chromex system was used instead of the Echelle system, in order to take advantage of the greater emission signals recorded using the former. Examination of the temporal dependence of Li(I) emission intensity as a function of pulse energy and pressure reveals several features. Increasing laser pulse energy is shown to have a significant effect on emission evolution: when using 60 mJ/pulse (as opposed to 30 mJ/pulse) the maximum emission intensity is significantly higher, occurs earlier in the plasma evolution, and is followed by more rapid emission decay. This dependence on laser pulse energy might be attributed to the fact that for increased pulse energy, plasma formation and thus plasma shielding occur earlier in time with respect to the laser pulse. Interestingly, increasing solution pressure also appears to affect emission evolution, and the maximum and minimum pressure effects appear at different points in time for the two different pulse energies. Note that with a pulse energy of 60 mJ/pulse and a gate delay of 200 ns, corresponding to the measurement conditions used to obtain the spectra in Figs. 2 and 3, the minimum pressure effect is observed (See Fig. 4b).

The pressure effect on emission line width was also briefly examined. Figure 5 shows a plot of FWHM of the unresolved Li(I) emission doublet (670.776 and 670.791 nm) for pressures ranging from 7×10^5 up to 2.76×10^7 Pa (7–276 bar). These measurements were made using a laser pulse energy of 30 mJ/pulse and different detector gate delays, 600 and 2000 ns, corresponding to the conditions at which the maximum and minimum pressure effects were observed (see Fig. 4a). Based

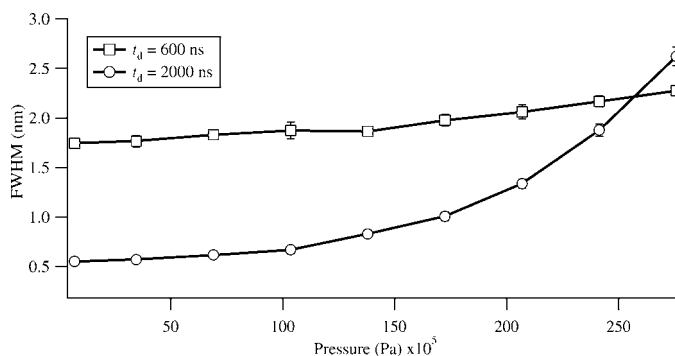


FIG. 5. Pressure dependence of the width (FWHM) of the Li(I) emission doublet (670.776 and 670.791 nm) measured at two different points in plasma evolution, (□) $t_d = 600$ ns and (○) $t_d = 2000$ ns, for pressures from 7×10^5 Pa to 2.76×10^7 Pa. Measurements were made using the Chromex system and $t_b = 1$ μ s. Pulse energy = 30 mJ/pulse. Error bars represent 1 standard deviation.

on the data shown in Fig. 5, it appears that pressure has a much larger effect on line width when measured at a later time in the plasma evolution ($t_d = 2000$ ns). This result might be attributed to the fact that as the plasma cools and expands (longer t_d values), the external pressure has a greater effect on the plasma, leading to reduced plasma volume and increased collisional broadening. Also, the increased collisional and Stark broadening inherent to the high-pressure (20–60 kbar), high-temperature (on the order of 10 000 K), and high-electron-density (10^{19} – 10^{20} /cm³)^{32,36} early-stage plasma dominates broadening caused by the elevated solution pressure, yielding much broader emission lines for all but the highest pressure shown (2.76×10^7 Pa, 276 bar) in Fig. 5. The results shown in Fig. 5 explain why pressure had little effect on the widths of the emission lines in the Echelle spectra shown in Figs. 2 and 3, considering they were measured using a very short gate delay ($t_d = 200$ ns). In addition to the work performed using 30 mJ/pulse, as shown in Fig. 5, similar investigations were also performed using 60 mJ/pulse, and the pressure effect on line width was observed to depend on the laser pulse energy (data not shown).

Although the purpose of this study was not to provide high-sensitivity LIBS measurements at elevated pressures, rough estimations of detection limits were made as a qualitative indication of the suitability of LIBS for *in situ* vent fluid measurements. The spectra shown in Fig. 2 were used to estimate detection limits of 5, 54, and 85 ppm for Li, Ca, and Mn, respectively. The detection limit for Na was not estimated, but is known to be on the sub-ppm level. The estimated detection limits are close to or within measured concentration ranges at the 9–10°N vent sites on the East Pacific Rise: Na, Li, Ca, and Mn were reported to vary between 253–15 000, 0.27–8.7, 40–1900, and 3–55 ppm, respectively.¹ However, other reports of LIBS for these elements in bulk solution found detection limits as low as 7.5, 13, and 130 ppb³⁴ for Na, Li, and Ca, respectively, and 3 ppm¹⁰ for Mn (measured using surface analysis). The detection limits estimated as part of this investigation are much higher than those reported in previous studies due to the fact that measurement conditions were not optimized to provide the highest sensitivity for each element, but were chosen so that all elements could be measured simultaneously with similar emission intensities. Additionally, the spectra were measured using a very low throughput $f/10$ echelle spectrometer.

CONCLUSION

The results reported in this paper, although not intended as systematic and exhaustive, demonstrate LIBS as a viable technique for detection of a range of dissolved ions at pressures comparable to those of hydrothermal vent sites. Based on rough estimations of sensitivity, it should be feasible to measure both alkali and alkaline earth metals such as Na, Li, and Ca, and with less certainty, trace metals such as Mn, in hydrothermal vent fluids. These studies also reveal that LIBS spectral features, specifically, emission intensity and line width, are affected by pressure, and that the observed pressure effects depend on experimental parameters, including the time at which emission is observed following the laser pulse and the laser pulse energy used for excitation. Future studies will utilize direct spectral imaging of the laser-induced plasma in the hopes of gaining additional insight into the effects of pressure on plasma dynamics. We are also investigating dual laser pulse LIBS (dual-pulse LIBS or DP-LIBS) for analysis of several analytes that were not easily detected using single-pulse excitation.

ACKNOWLEDGMENT

We would like to thank the National Science Foundation for support of this work under grant numbers OCE-0352242, OCE-0527927, and CHE-0316069.

1. K. L. Von Damm, "Controls on the Chemistry and Temporal Variability of Seafloor Hydrothermal Fluids", in *Seafloor Hydrothermal Systems: Physical, Chemical, Biological, and Geological Interactions*, S. E. Humphris, R. A. Zierenberg, L. S. Mullineaux, and R. E. Thomson, Eds. (Geophysical Monograph Series, American Geophysical Union, Washington, D.C., 1995), Chap. 91, p. 222.
2. K. L. Daly, R. H. Byrne, A. G. Dickson, S. M. Gallagher, M. J. Perry, and M. K. Tivey, *Marine Tech. Soc. J.* **38**(2), 121 (2004).
3. S. M. Gallagher and J. Whelan, Eds. "The Next Generation of In Situ Biological and Chemical Sensors in the Ocean: A Workshop Report" (www.whoi.edu/institutes/oli/images/final_report.pdf, accessed 2004).
4. P. F. Lonsdale, *Deep-Sea Research* **24**, 857 (1977).
5. F. Brech and L. Cross, *Appl. Spectrosc.* **16**, 59 (1962).
6. D. A. Cremers, *Appl. Spectrosc.* **41**, 572 (1987).
7. C. M. Davies, H. H. Telle, D. J. Montgomery, and R. E. Corbett, *Spectrochim. Acta, Part B* **50**, 1059 (1995).
8. B. J. Marquardt, S. R. Goode, and S. M. Angel, *Anal. Chem.* **68**, 977 (1996).
9. B. J. Marquardt, D. N. Stratis, D. A. Cremers, and S. M. Angel, *Appl. Spectrosc.* **52**, 1148 (1998).
10. O. Samek, D. C. S. Beddows, J. Kaiser, S. V. Kukhlevsky, M. Liška, H. H. Telle, and J. Young, *Opt. Eng.* **39**, 2248 (2000).
11. H. H. Telle, D. C. S. Beddows, G. W. Morris, and O. Samek, *Spectrochim. Acta, Part B* **56**, 947 (2001).
12. S. Palanco, J. M. Baena, and J. J. Laserna, *Spectrochim. Acta, Part B* **57**, 591 (2002).
13. R. C. Wiens, S. K. Sharma, J. Thompson, A. Misra, and P. G. Lucey, *Spectrochim. Acta, Part A* **61**, 2324 (2005).
14. J. D. Blacic, D. R. Pettit, D. A. Cremers, and N. Roessler, "Laser-Induced Breakdown Spectroscopy for Remote Elemental Analysis of Planetary Surfaces", *Proceedings of the International Symposium on Spectral Sensing Research*, 302 (1992).
15. C. M. Davies, H. H. Telle, and A. W. Williams, *Fresenius' J. Anal. Chem.* **355**, 895 (1996).
16. X. D. Hou and B. T. Jones, *Microchem. J.* **66**, 115 (2000).
17. A. K. Knight, N. L. Scherbarth, D. A. Cremers, and M. J. Ferris, *Appl. Spectrosc.* **54**, 331 (2000).
18. J. Gruber, J. Heitz, H. Strasser, D. Bäuerle, and N. Ramaseder, *Spectrochim. Acta, Part B* **56**, 685 (2001).
19. A. I. Whitehouse, J. Young, I. M. Botheroyd, S. Lawson, C. P. Evans, and J. Wright, *Spectrochim. Acta, Part B* **56**, 821 (2001).
20. Z. A. Arp, D. A. Cremers, R. D. Harris, D. M. Oschwald, G. R. Parker, Jr., and D. M. Wayne, *Spectrochim. Acta, Part B* **59**, 987 (2004).
21. C. López-Moreno, S. Palanco, and J. J. Laserna, *Spectrochim. Acta, Part B* **60**, 1034 (2005).
22. S. Koch, R. Court, W. Garen, W. Neu, and R. Reuter, *Spectrochim. Acta, Part B* **60**, 1230 (2005).
23. L. Paksy, B. Németh, A. Lengyel, L. Kozma, and J. Czakkel, *Spectrochim. Acta, Part B* **51**, 279 (1996).
24. M. Tran, Q. Sun, B. Smith, and J. D. Winefordner, *Anal. Chim. Acta* **419**, 153 (2000).
25. R. T. Wainner, R. S. Harmon, A. W. Miziolek, K. L. McNesby, and P. D. French, *Spectrochim. Acta, Part B* **56**, 777 (2001).
26. R. Barbini, F. Colao, V. Lazic, R. Fantoni, A. Palucci, and M. Angelone, *Spectrochim. Acta, Part B* **57**, 1203 (2002).
27. D. Bulajic, G. Cristoforetti, M. Corsi, M. Hidalgo, S. Legnaioli, V. Palleschi, A. Salvetti, E. Tognoni, S. Green, D. Bates, A. Steiger, J. Fonseca, J. Martins, J. McKay, B. Tozer, D. Wells, R. Wells, and M. A. Harith, *Spectrochim. Acta, Part B* **57**, 1181 (2002).
28. M. Noda, Y. Deguchi, S. Iwasaki, and N. Yoshikawa, *Spectrochim. Acta, Part B* **57**, 701 (2002).
29. W. B. Lee, J. Wu, Y. I. Lee, and J. Sneddon, *Appl. Spectrosc.* **39**, 27 (2004).
30. C. A. Munson, F. C. De Lucia, Jr., T. Piehler, K. L. McNesby, and A. W. Miziolek, *Spectrochim. Acta, Part B* **60**, 1217 (2005).
31. B. Sallé, D. A. Cremers, S. Maurice, and R. C. Wiens, *Spectrochim. Acta, Part B* **60**, 479 (2005).
32. D. A. Cremers, L. J. Radziemski, and T. R. Loree, *Appl. Spectrosc.* **38**, 721 (1984).
33. R. Nyga and W. Neu, *Opt. Lett.* **18**, 747 (1993).
34. R. Knopp, F. J. Scherbaum, and J. T. Kim, *Fresenius' J. Anal. Chem.* **355**, 16 (1996).
35. A. E. Pichahchy, D. A. Cremers, and M. J. Ferris, *Spectrochim. Acta, Part B* **52**, 25 (1997).
36. P. K. Kennedy, D. X. Hammer, and B. A. Rockwell, *Prog. Quant. Electron* **21**(3), 155 (1997).
37. D. C. S. Beddows, O. Samek, M. Liska, and H. H. Telle, *Spectrochim. Acta, Part B* **57**, 1461 (2002).
38. W. F. Pearman, J. Scaffidi, and S. M. Angel, "Trace Metal Analysis in Bulk Aqueous solution using nanosecond dual pulse laser induced breakdown spectroscopy", in *Trends in Optics and Photonics Book Series, Book 81 (Laser Induced Plasma Spectroscopy and Applications)* (Optical Society of America, Washington, D.C., 2002), p. 218.
39. W. Pearman, J. Scaffidi, and S. M. Angel, *Appl. Opt.* **42**, 6085 (2003).
40. S. Koch, W. Garen, M. Müller, and W. Neu, *Appl. Phys. A* **79**, 1071 (2004).
41. L. St-Onge, E. Kwong, M. Sabsabi, and E. B. Vadas, *J. Pharm. Biomed. Anal.* **36**, 277 (2004).
42. A. De Giacomo, M. Dell'Aglio, F. Colao, and R. Fantoni, *Spectrochim. Acta, Part B* **59**, 1431 (2004).
43. A. De Giacomo, M. Dell'Aglio, and O. De Pascale, *Appl. Phys. A* **79**, 1035 (2004).
44. A. De Giacomo, M. Dell'Aglio, F. Colao, R. Fantoni, and V. Lazic, *Appl. Surf. Sci.* **247**, 157 (2005).
45. A. Casavola, A. De Giacomo, M. Dell'Aglio, F. Taccogna, G. Colonna, O. De Pascale, and S. Longo, *Spectrochim. Acta, Part B* **60**, 975 (2005).
46. V. Lazic, F. Colao, R. Fantoni, and V. Spizzicchino, *Spectrochim. Acta, Part B* **60**, 1002 (2005).
47. V. Lazic, F. Colao, R. Fantoni, and V. Spizzicchino, *Spectrochim. Acta, Part B* **60**, 1014 (2005).
48. S. Nakamura, Y. Ito, and K. Sone, *Anal. Chem.* **68**, 2981 (1996).
49. L. J. Radziemski, T. R. Loree, D. A. Cremers, and N. M. Hoffman, *Anal. Chem.* **55**, 1246 (1983).
50. X. Mao, X. Zeng, S. B. Wen, and R. E. Russo, *Spectrochim. Acta, Part B* **60**, 960 (2005).
51. V. Detalle, R. Héon, M. Sabsabi, and L. St-Onge, *Spectrochim. Acta, Part B* **56**, 1011 (2001).